



## Bone Regeneration Using the Freshly Isolated Autologous Stromal Vascular Fraction of Adipose Tissue in Combination With Calcium Phosphate Ceramics

HENK-JAN PRINS,<sup>a,b,\*</sup> ENGELBERT A.J.M. SCHULTEN,<sup>b,\*</sup> CHRISTIAAN M. TEN BRUGGENKATE,<sup>b</sup> JENNEKE KLEIN-NULEND,<sup>a,†</sup> MARCO N. HELDER<sup>c,†</sup>

**Key Words.** Bone regeneration • Clinical study • Calcium phosphates • Maxillary sinus floor elevation • Adipose stem cells • Regenerative medicine

### ABSTRACT

In patients undergoing maxillary sinus floor elevation (MSFE) for dental implant placement, bone substitutes are currently evaluated as alternatives for autologous bone. However, bone substitutes have only osteoconductive properties and lack osteoinductive potential. Therefore, this phase I study evaluated the potential additive effect on bone regeneration by the addition of freshly isolated, autologous but heterologous stromal vascular fraction (SVF), which is highly enriched with adipose stromal/stem cells when compared with native adipose tissue. From 10 patients, SVF was procured using automatic processing, seeded on either  $\beta$ -tricalcium phosphate ( $n = 5$ ) or biphasic calcium phosphate carriers ( $n = 5$ ), and used for MSFE in a one-step surgical procedure. Primary objectives were feasibility and safety. The secondary objective was efficacy, evaluated by using biopsies of the augmented area taken 6 months postoperatively, concomitant with dental implant placement. Biopsies were assessed for bone, graft, and osteoid volumes. No adverse effects were reported during the procedure or follow-up ( $\geq 3$  years). Bone and osteoid percentages were higher in study biopsies (SVF supplemented) than in control biopsies (ceramic only on contralateral side), in particular in  $\beta$ -tricalcium phosphate-treated patients. Paired analysis on the six bilaterally treated patients revealed markedly higher bone and osteoid volumes using microcomputed tomography or histomorphometric evaluations, demonstrating an additive effect of SVF supplementation, independent of the bone substitute. This study demonstrated for the first time the feasibility, safety, and potential efficacy of SVF seeded on bone substitutes for MSFE, providing the first step toward a novel treatment concept that might offer broad potential for SVF-based regenerative medicine applications. *STEM CELLS TRANSLATIONAL MEDICINE* 2016;5:1–13

### SIGNIFICANCE

This is the first-in-human study using freshly isolated, autologous adipose stem cell preparations (the stromal vascular fraction [SVF] of adipose tissue) applied in a one-step surgical procedure with calcium phosphate ceramics (CaP) to increase maxillary bone height for dental implantations. All 10 patients received CaP plus SVF on one side, whereas bilaterally treated patients (6 of 10) received CaP only on the opposite side. This allowed inpatient evaluation of the potential added value of SVF supplementation, assessed in biopsies obtained after 6 months. Feasibility, safety, and potential efficacy of SVF for bone regeneration were demonstrated, showing high potential for this novel concept.

### INTRODUCTION

Bone regeneration for bone defect treatment in the oral and maxillofacial region remains challenging. Insufficient alveolar bone height in the lateral maxilla is a limiting factor for placing dental implants. These cases are currently treated with a maxillary sinus floor elevation (MSFE) procedure, using predominantly mandibular or iliac crest bone to increase bone volume [1]. The use of

autologous bone remains the gold standard, because it has osteoconductive as well as osteoinductive properties, contains osteogenic cells, and does not evoke immunogenic responses. The drawbacks of using autologous bone, essentially caused by the harvesting procedure, encourages the search for alternative strategies. Other types of graft materials used to augment bone volume enabling dental implant placement include allogeneic bone, demineralized bone

<sup>a</sup>Department of Oral Cell Biology, Academic Centre for Dentistry Amsterdam (ACTA), MOVE Research Institute, VU University Amsterdam, Amsterdam, The Netherlands; <sup>b</sup>Department of Oral and Maxillofacial Surgery, MOVE Research Institute Amsterdam, VU University Medical Center/ACTA, Amsterdam, The Netherlands; <sup>c</sup>Department of Orthopedic Surgery, MOVE Research Institute Amsterdam, VU University Medical Center, Amsterdam, The Netherlands

\* Contributed equally as primary authors.

† Contributed equally as last authors.

Correspondence: Marco N. Helder, Ph.D., Department of Orthopedic Surgery, VU University Medical Center, De Boelelaan 1117, 1081 HV Amsterdam, The Netherlands. Telephone: 31 204445024; E-mail: m.helder@vumc.nl

Received December 2, 2015; accepted for publication April 18, 2016.

©AlphaMed Press  
1066-5099/2016/\$20.00/0

<http://dx.doi.org/10.5966/sctm.2015-0369>

matrices, and several synthetic biomaterials such as ceramics and polymers, or combinations of graft materials [2]. A meta-analysis demonstrated that  $\beta$ -tricalcium phosphate ( $\beta$ -TCP) as graft material for MSFE results in the highest total bone volume when compared with other graft materials but is still inferior to autologous bone [3].  $\beta$ -TCP is biodegradable and can be replaced by bone, but the degradation rate might be too high for low bone in-growth rates. Therefore, biphasic calcium phosphates (BCP), consisting of  $\beta$ -TCP with the less soluble hydroxyapatite (HA), might be more effective in the balance between calcium phosphate degradation and bone in-growth/replacement.

Calcium phosphate carriers show low bone in-growth rates in comparison with autologous bone grafts [4, 5]. This low bone in-growth results from a lack of osteoinductive potential, because calcium phosphate carriers have only osteoconductive properties, which depend on bone in-growth from the pre-existing (native) bone in the maxillary sinus floor [5]. Cell-based bone tissue engineering is a promising strategy to improve bone formation by providing osteogenic cells and secretion of osteoinductive signals to recruit cells from the surrounding bone tissue [6, 7]. This might result in sufficient bone regeneration within a shorter time period than is required when using bone substitutes only.

Adult bone marrow-derived mesenchymal stem cells (BMSCs) are the most frequently used cells in cell-based bone tissue engineering. However, the frequency of BMSCs in human bone marrow is rather low (0.001%–0.01%) [8]. Expansion of BMSCs is required for clinical application, for which large numbers of cells are needed, *id est* in the range of  $1\text{--}20 \times 10^8$  cells for systemic applications [9–11]. Cell expansion for clinical application needs to be done in a laborious, expensive, and time-consuming good manufacturing practice (GMP) laboratory. Unfortunately, BMSCs lose their proliferative and differentiation capacity during cell expansion [12–14], and there is also an increased risk for pathogen contamination and genetic transformation [15, 16].

Adipose tissue-derived mesenchymal stem cells (ASCs) have opened appealing new possibilities in adult stem cell therapies. ASCs show many similarities with BMSCs with regard to surface marker profiles, multilineage potential, and growth properties [17, 18]. However, in contrast to bone marrow, adipose tissue has the following advantages: (a) it can be harvested with minimal patient discomfort, (b) it contains a high stem cell to volume ratio [17, 19–23], (c) harvesting can easily be upscaled according to the need, and (d) it can be processed within a short time frame to obtain highly enriched ASC preparations (residing in the stromal vascular fraction [SVF]). At least, the multipotent cells within the SVF attach very fast to the scaffold material, proliferate rapidly, and can be differentiated toward the osteogenic lineage [24, 25]. Taken together, this allows one to obtain clinically relevant stem cell-like cell quantities that can be applied immediately after adipose tissue processing in a previously described so-called one-step surgical procedure [2, 26].

A one-step surgical procedure enables the use of minimally manipulated cells. This way, many regulatory hurdles are avoided, thereby accelerating the development of new medical solutions in clinical practice and minimizing the risks induced by culturing cells as described above [12–16]. Earlier, we showed the feasibility of a one-step surgical procedure in preclinical animal studies [27, 28]. The translation of this concept into a clinical trial was a logical next step. The MSFE model provides a unique opportunity to accurately and precisely assess bone formation after MSFE, by taking bone biopsies prior to dental implant placement [2, 5],

and allows inpatient comparison of treatment modalities using a “split-mouth” design [29]. Therefore, in this study the MSFE model was used to investigate the feasibility, safety, and efficacy of a one-step surgical procedure in a clinical setting by combining calcium phosphate carriers with autologous SVF.

## MATERIALS AND METHODS

### Study Approval

This study, registered in the Netherlands Trial Registry (NTR4408; <http://www.trialregister.nl>), was conducted with the approval of the medical ethical committee of the Vrije Universiteit (VU) Amsterdam university medical center, as well as the Central Committee on Research Involving Human Subjects (The Hague, The Netherlands; Dossier number: NL29581.000.09; EudraCT-number: 2009-015562-62). All patients signed a written informed consent before participation in the study. This study complied with the principles of the Declaration of Helsinki.

### Patient Selection

Ten patients were included in this study, who were partially edentulous in the posterior maxilla and required dental implants for prosthetic rehabilitation. All patients had an adequate alveolar bone height of at least 4 mm, but not more than 8 mm at the lateral maxilla. Therefore, a preoperative panoramic radiograph was made and carefully examined for contour lines of the maxillary sinus floor and to determine the preoperative bone height at the planned dental implant positions. The average age of the patient group was  $56 \pm 7$  years (range: 46–69 years). The mean body mass index (BMI) was  $29.3 \pm 3.8$ ; three patients (30%) were lean (BMI < 25), one patient (10%) was overweight, and six patients (60%) were obese (BMI > 30). Six patients were females and four were males (Table 1). All patients were nonsmokers. Patients younger than 18 years or with specific conditions—such as systemic diseases, malignancies, chronic infections, immune system abnormalities, cardiovascular diseases, drug abuse, and pregnancy—were excluded from participation in the study. Patients who required horizontal bone augmentation, as well as patients using nonsteroidal anti-inflammatory drugs within 15 days before surgery, were also excluded from this study. A patient’s flowchart is shown in supplemental online Figure 1, and all procedures and assessments according to the study protocol are summarized in supplemental online Table 1.

### Safety Measurements

For determination of safety, all patients were monitored for general health changes and (serious) adverse events related to the product or procedure at each visit during the study (supplemental online Table 1). Radiological assessments (panoramic radiographs and cone beam-computerized tomography [CT] scans) were carefully screened for any remarkable deviations. Physical examination consisted of inspection or determination of general appearance, weight, blood pressure, pulse rate, skin, lymph nodes, thyroid, musculoskeletal system and extremities, cardiovascular system, lungs, abdomen, and neurological status. Blood laboratory safety measurements consisted of the assessment of hematological parameters, including erythrocyte count, white blood cell count, hematocrit, hemoglobin concentration, eosinophil count, basophil counts, lymphocyte count, neutrophil count, monocyte and thrombocyte counts, as well as serum chemistry measurements, including

**Table 1.** Patient data

Patient number	Gender, age (years)	Body mass index	Unilateral/bilateral	Control/study side	Graft material	Dental implant positions
1	♀, 58	24.5	Bilateral	Control Study	$\beta$ -TCP	14, 15, <b>16</b> 24, 25, <b>26</b>
2	♀, 46	30.4	Bilateral	Study Control	$\beta$ -TCP	14, <b>15</b> , 16 24, 25, <b>26</b>
3	♂, 69	35.8	Bilateral	Control Study	$\beta$ -TCP	14, 15, <b>16</b> 25, 26, <b>27</b>
4	♀, 59	31.2	Unilateral	Study	$\beta$ -TCP	24, <b>25</b> , 26
5	♂, 64	24.8	Unilateral	Study	$\beta$ -TCP	15, <b>16</b>
6	♀, 57	24.2	Bilateral	Study Control	BCP	14, 15, <b>16</b> 24, <b>26</b>
7	♂, 56	28.7	Bilateral	Study Control	BCP	15, 16, <b>17</b> 25, <b>26</b> , 27
8	♀, 51	30.9	Unilateral	Study	BCP	14, <b>15</b> , 16
9	♂, 52	32.1	Unilateral	Study	BCP	23, 25, <b>26</b>
10	♀, 51	30.3	Bilateral	Study Control	BCP	15, <b>16</b> 25, <b>26</b>

Gender and age, body mass index, whether the patients were treated unilaterally or bilaterally (“split-mouth design”), bone substitute used to augment bone of the maxillary sinus floor, and the dental implant sites are given according to the Fédération Dentaire Internationale system. Selected biopsies are displayed in boldface type.

Abbreviations: BCP, biphasic calcium phosphate;  $\beta$ -TCP,  $\beta$ -tricalcium phosphate.

alanine aminotransferase, aspartate aminotransferase, total bilirubin,  $\gamma$ -glutamyl transferase, alkaline phosphatase, lactate dehydrogenase, amylase, lipase, albumin, total protein, glucose, creatinine, uric acid, calcium, potassium, sodium, urea nitrogen, creatinine kinase, c-reactive protein, and human chorionic gonadotropin (if applicable).

## One-Step Surgical Procedure

### Collection of Adipose Tissue

Patients were brought under general anesthesia prior to the surgery. To obtain adipose tissue, a plastic surgeon performed a syringe-based lipoaspiration. To this end, a 14-gauge, 2-mm diameter, blunt-end disposable infusion needle (Cloverleaf Medical, Buckinghamshire, UK; <http://www.ibuckinghamshire.co.uk/>) was used for tumescent fluid infiltration, which consisted of 0.9% sodium chloride solution, supplemented with 10  $\mu$ g/ml adrenalin, 0.02% bupivacain, and 0.05% sodium hydrogen. After 15 minutes' incubation, adipose tissue was obtained manually from the abdominal wall using an aspiration 3-mm cannula with a Mercedes tip (Cloverleaf Medical) connected to a 60-ml Toomey syringe (GE Healthcare, Buckinghamshire, UK; [www.gehealthcare.com](http://www.gehealthcare.com)) (Fig. 1A). By placing the filled syringes in a vertical position, we found that two distinct layers appear: a top layer containing adipose tissue and a bottom layer consisting of blood, waste, and tumescent fluid (Fig. 1B). Liposuction was continued until 150 ml or more adipose tissue was harvested. The small surgical incisions were closed with intracutaneous absorbable Monocryl 5-0 (Ethicon; Johnson & Johnson International, Diegem, Belgium; [www.jnj.com](http://www.jnj.com)), and a pressure bandage (Tubigrip) was applied.

### Cell Isolation, Counting, and Construct Preparation

The syringes filled with adipose tissue were transported to a special stem cell laboratory within the VU University medical center

operation complex. Within the stem cell laboratory, the adipose tissue was transferred to a Celution 800/CRS device (Cytori Therapeutics, Inc., San Diego, CA, USA; <http://www.cytori.com/>) (Fig. 1C) for automated and standardized extraction, washing, and concentration of the patient's own adipose-derived SVF according to the manufacturer's protocol (Celution 800/CRS software, version 4.1; Cytori Therapeutics, San Diego, CA, <http://www.cytori.com>), resulting in 5 ml of cell suspension. Viability and cell number were determined in triplicate with a Nucleocounter NC-100 (ChemoMetec A/S, Allerød, Denmark; <https://chemometec.com/>), according to manufacturer's protocol. Briefly, a 1:50 diluted sample was measured in triplicate using propidium iodide containing nucleocassettes (ChemoMetec) to determine the number of dead cells per milliliter. Subsequently, 100  $\mu$ l of the 1:50 diluted sample was lysed by adding the same volume of Reagent A100 (ChemoMetec; pH 1.25), stabilized with the same volume of Reagent B, and measured in triplicate to determine the total cell number per milliliter. The viable cell number per milliliter was calculated by subtracting the mean dead cell number per milliliter from the mean total cell number. Release criterion was set at  $\geq 70\%$  viability. Then  $7.5 \times 10^6$  cells per milliliter of Ringer's lactate solution were seeded onto 100% Ceros  $\beta$ -TCP with 60% porosity and granule size of 0.7–1.4 mm (Thommen Medical, Grenchen, Switzerland; <http://www.thommenmedical.com/>) or Straumann Bone Ceramic BCP, consisting of 60% hydroxyapatite and 40%  $\beta$ -TCP with 90% porosity and granule size of 0.5–1.0 mm (Straumann, Basel, Switzerland; <http://www.straumann.com/>). For each maxillary sinus, we prepared 2 g calcium phosphate carrier with  $20 \times 10^6$  cells (2.67 ml of the  $7.5 \times 10^6$  cells per milliliter). Cells were incubated on the carrier material for 30 minutes at room temperature (RT) (Fig. 1D). After two washing steps of 5 minutes with Ringer's lactate solution, the constructs of calcium phosphate carrier with or without SVF were transported back to the operation room. In case of a bilateral “split-mouth” design treatment with calcium phosphate carrier combined with SVF

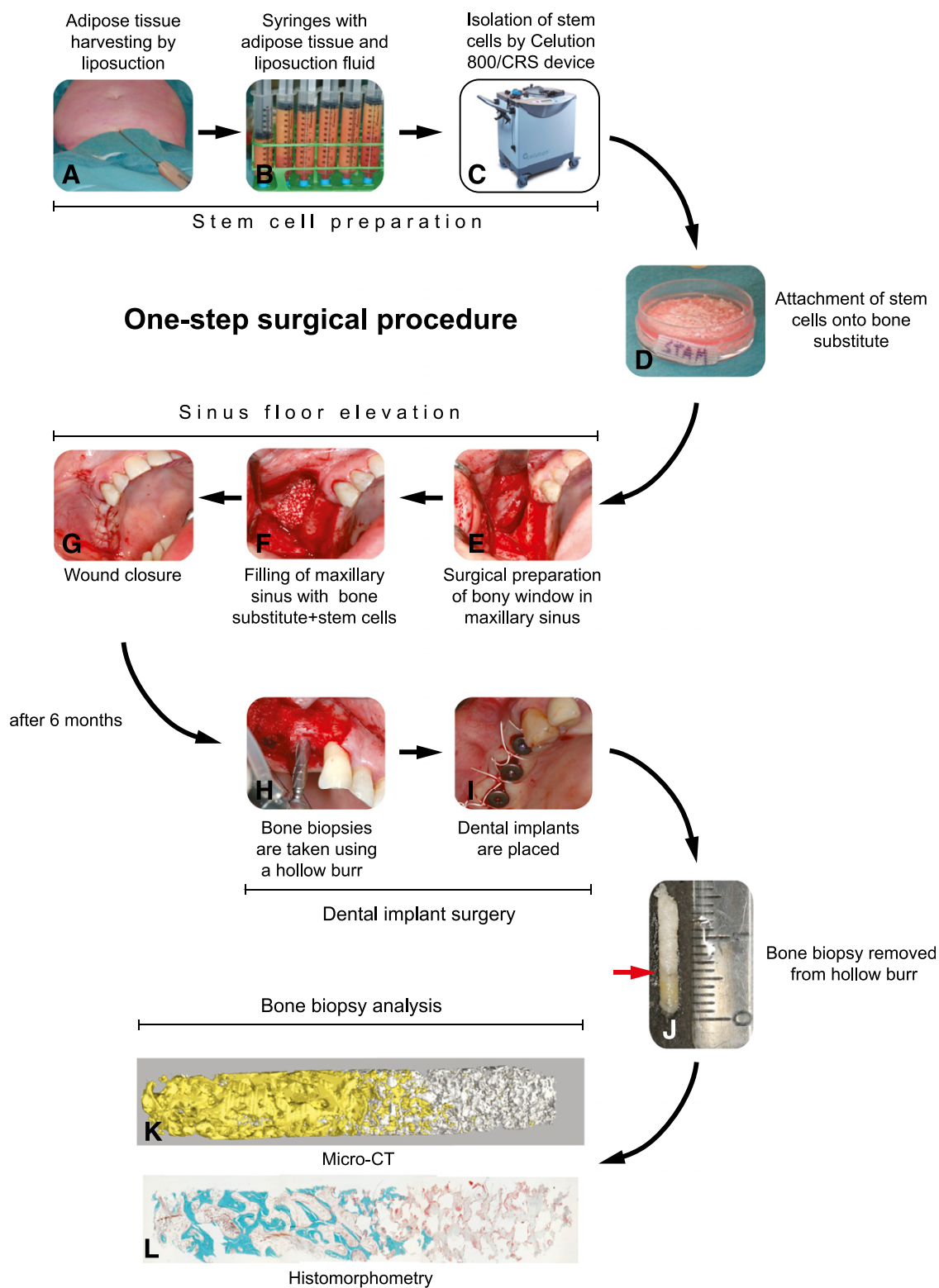


**Figure 1.** Schematic overview of one-step surgical procedure, maxillary sinus floor elevation, and biopsy analysis. **(A):** The plastic surgeon starts harvesting adipose tissue by liposuction. **(B):** The adipose tissue and liposuction fluid is collected in syringes. **(C):** The filled syringes are transferred into a Celution 800/CRS system. This device washes, digests, and centrifugates the adipose tissue to obtain the fresh stromal vascular fraction containing the adipose stem cells. After isolation of the stromal vascular fraction, cells can be shortly stimulated with the growth factors before seeding the stimulated cells onto a carrier material. **(D):** The freshly isolated adipose stem cells are seeded onto the calcium phosphate carrier. Unattached cells are washed off ("stam"=stem cells). **(E):** During the short attachment period of the cells (30 minutes), the patient is prepared for the maxillary sinus floor elevation procedure via a lateral approach. After reflection of the mucoperiosteal flap, a bony window is (Figure legend continues on next page.)

on the study side and calcium phosphate carrier only at the control side, the control samples were treated with Ringer's lactate solution only.

### Maxillary Sinus Floor Elevation

The MSFE procedure was performed as previously described [5, 30]. In short, a lateral bony window was prepared and turned inward and upward (Fig. 1E), and the generated cavity within the maxillary sinus was filled with calcium phosphate carrier alone (control side) or calcium phosphate carrier with SVF (study side) (Fig. 1F), and the wound was closed with Vicryl Plus 3 × 0 sutures (Ethicon, Johnson & Johnson International) (Fig. 1G). Surplus material was fixated in 4% formaldehyde solution (Klinipath BV, Duiven, The Netherlands; <http://www.klinipath.nl/>). No collagenous barrier membrane was used to cover the lateral window [5]. The sutures were removed after 10–14 days. All patients received preoperative antibiotic prophylaxis, consisting of 500 mg amoxicillin 3 times daily and for 7 days postoperatively. After a healing period of 5 months post-MSFE (prior to dental implant placement), a panoramic radiograph was made to determine the increase in vertical height bone + bone substitute at the planned dental implant positions.

### Dental Implant Surgery

Six months after the MSFE procedure, dental implant surgery was performed under local anesthesia. A crestal incision was made with mesial and distal buccal vertical release incisions. A full-thickness mucoperiosteal flap was raised to expose the underlying alveolar ridge, which was inspected for sufficient bone volume for the intended dental implant placement. Then implant preparations were made and biopsies were collected with a hollow trephine drill (Fig. 1H) with an external diameter of 3.5 mm (Straumann AG) and using sterile saline for copious irrigation. Straumann dental implants with a diameter of 4.1 mm, a length of 10 or 12 mm, and a sand-blasted, large-grit, acid-etched surface were placed in the augmented maxillary sinus. Dental implants were placed in a single-stage surgical procedure, mounted with healing caps, and sutured with Gore-Tex sutures (W.L. Gore and Associates, Newark, DE, USA; <http://www.gore.com/>) (Fig. 1I). Immediately after dental implant placement (6 months post-MSFE) another panoramic radiograph was made to check dental implant placement. The panoramic radiographs (pre-MSFE, as well as before dental implant placement) were used for morphometric measurements to determine the vertical bone + bone substitute height at the planned implant positions, using digital software. Calculations were performed with the use of a conversion factor that adjusted for magnification of the panoramic radiograph.

Sutures were removed after 10–14 days. Patients were instructed to avoid loading of the dental implants during the postimplant surgical osseointegration time. After a 3-month osseointegration period, the superstructures were manufactured and placed by the patient's dentist.

### Colony-Forming Unit Fibroblast Assay and Cell Expansion

To determine retrospectively the stem cell frequency within the SVF, we seeded cells in a colony-forming unit fibroblast (CFU-F) assay. SVF cells were seeded in the concentrations  $25 \times 10^3$ ,  $10 \times 10^3$ ,  $4 \times 10^3$ ,  $1.6 \times 10^3$ ,  $0.8 \times 10^3$ , and  $0.4 \times 10^3$  cells per well in triplicate in six-well plates in expansion medium supplemented with 5% human platelet lysate, as previously described [31, 32]. After 14 days, colonies were fixated with 4% formalin for 15 minutes, stained with 0.2% toluidine blue solution for 10 minutes at RT, and washed twice with distilled H<sub>2</sub>O. CFU-F colonies containing at least 50 cells were scored using a microscope, and the frequency of the colonies was calculated. Confluent wells were excluded, and mean frequencies were calculated from the wells in which separate colonies were distinguishable. For expansion,  $1 \times 10^5$  cells/cm<sup>2</sup> were seeded and cultured in expansion medium. Expanded ASCs were harvested using trypsin and stored in liquid nitrogen for further analyses.

### Fluorescent Cell Nuclei Staining and Scanning Electron Microscopy

To determine whether cells attached to the calcium phosphate carrier, we fluorescently stained fixated constructs (calcium phosphate carriers with seeded cells) by using 4',6-diamidino-2-phenylindole (DAPI) and visualized by scanning electron microscopy. For fluorescent staining, constructs were washed twice with phosphate-buffered saline (PBS), and stained for 15 minutes with DAPI in a 1:50 dilution at RT. Subsequently, constructs were washed twice and visualized using fluorescence microscopy. For scanning electron microscopy, fixed constructs were dehydrated using a series of ethanol, immersed in hexamethyldisilazane twice for 30 min, air dried, mounted on scanning electron microscopy stubs, and immediately sputter-coated with gold before imaging the construct with a high-resolution JEOL scanning electron microscope (JEOL XL Series, 10 Kv, JEOL, Peabody, MA, USA, <http://www.jeolusa.com/>; Philips SEM XL 20, SEMTech Solutions, Eindhoven, The Netherlands, <http://www.semtechsolutions.com/>).

### Monoclonal Antibody Labeling and Flow Cytometry

The stromal vascular cell fraction (after one freeze-thaw cycle) and culture-expanded ASCs (passage 1; 10–14 days of culture) were analyzed for cell surface marker expression by using monoclonal antibodies against human CD29/ $\beta$ 1 integrin (555443), CD31/PECAM (555445), CD34 (345801), CD45 (555483), CD54 (555511), CD73/SH3 (550257), CD90/Thy-1 (555595), CD105/SH2 (560839), CD106/VCAM (555647), CD117/c-kit (555714), HLA-ABC (555552), HLA-DR (555811), and Lin1, including CD3, CD14, CD16, CD19, CD20, CD56 (340546) (all from BD Biosciences, San José, CA, USA; <https://www.bdbiosciences.com>), and CD166 (ALCAM, MCA1926F, AbD SeroTec/MorphoSys, Oxford, UK; <https://www.abdserotec.com>). All monoclonal antibodies used

(Figure legend continued from previous page.)

created in the lateral wall of the maxillary sinus and carefully moved and rotated medially toward the maxillary sinus, after dissection of the maxillary sinus mucosa (trap-door technique). (F): The tissue-engineered construct is inserted immediately into the patient, and the space created is filled with the bone substitute combined with the adipose stem cells. (G): Finally, the wound is closed. (H): After 6 months, bone biopsies are taken by using a hollow burr, and dental implants are placed (I). (J): Bone biopsies are removed from the hollow burr and analyzed by using micro-computed tomography (micro-CT) evaluation (K) and histomorphometry (L).

were of the IgG<sub>1</sub> type and either fluorescein isothiocyanate (FITC) or phycoerythrin (PE) conjugated. Cells were washed with PBS and stained with specific antibodies for 30 minutes at 4°C. Non-specific fluorescence was determined by incubating cells with isotype conjugated monoclonal antibodies antihuman IgG1-FITC and IgG1-PE (555748, 345816; BD Biosciences). Samples were washed twice and analyzed for surface marker expression in a FACSCaliber flow cytometer with the Cellquest Pro software (BD Biosciences). Expression of the markers was ranked as follows: -, <1%; ±, 1%–15%; +, 15%–95%; and ++, >95% positive cells.

### Biopsy Analysis

The bone biopsies taken during dental implant surgery with a hollow trephine drill were fixated in 4% phosphate-buffered formaldehyde (Klinipath BV), removed from the drill, transferred to 70% ethanol, and stored until use for micro-computed tomography (micro-CT) analysis (Fig. 1K; supplemental online Fig. 2A) and histomorphometric analysis (Fig. 1L; supplemental online Fig. 2B), as described below. For a valid uniform comparison of the biopsies taken from the sides that were treated with calcium phosphate only and the biopsies taken from the sides augmented with calcium phosphate and SVF, a selection was made by two independent experienced observers. The biopsies taken from implant sides outside the augmented maxillary sinus (mainly implant positions 14, 24, or both) were excluded from analysis. Per patient, one biopsy from each side was selected in the middle of the grafted area to exclude the effect of surrounding bone containing mechanically loaded dental elements and bone near the nasal wall of the maxillary sinus (Table 1).

### Micro-CT Analysis

Biopsies were kept in 70% ethanol, and three-dimensional (3D) biopsy reconstructions were obtained with a high-resolution micro-CT system ( $\mu$ CT 40; Scanco Medical AG, Bassersdorf, Switzerland; <http://www.scanco.ch/>). To this end, we fixed biopsies in synthetic foam, placed vertically in a polyetherimide holder, and scanned them at an isotropic voxel size of 10  $\mu$ m, source voltage of 70 kV, and current of 113  $\mu$ A. Gray values, depending on radiopacity of the scanned material, were converted into corresponding values of degree of mineralization by the analysis software (Scanco Medical AG). The distinction between newly formed bone and graft material was made by using the highest value of the degree of mineralization in the pre-existing sinus floor bone as threshold value. A distinction could be made between the original non-grafted native bone of the residual maxillary sinus floor and the graft material, because the mineralization degree of the graft material was significantly higher than was the mineralization degree of bone. A low threshold of 650 mg HA/cm<sup>3</sup> to distinguish bone tissue from connective tissue and bone marrow, and a high threshold of 270% was defined to distinguish graft material from bone tissue. These two thresholds were calculated by averaging the thresholds determined by two independent observers in three slices of three bone biopsies. Similar thresholds were defined for  $\beta$ -TCP and BCP. Using this simple thresholding resulted initially in the detection of a thin layer of nonexistent “bone” covering the graft material throughout the grafted area of the sinus. Therefore, a new and so-called “onion-peeling” algorithm (Scanco Medical AG) was used to discriminate between the newly formed bone deposited on the graft material and the graft material itself. This method peels off voxels from the thin layer of

“bone” (as measured with the simple thresholding method) and removes this layer when calcium phosphate is detected within a predefined extent of space. The digital images of the scanned biopsies were analyzed, starting from the caudal side of the biopsy, and continuing toward the cranial side. Regions of interest (ROIs) of 1 mm thickness were defined as previously described [5]. A comparison was made between the results of the total biopsies taken from the control sides without stem cells and study sides with stem cells. Additionally, to obtain more insight into where the bone was formed within the grafted area, we pooled the bone volumes obtained from the ROI in the residual native bone parts, whereby the ROIs were numbered in a consecutive sequence starting from the residual sinus floor up to the most cranial part of the biopsy. These volumes of interest were analyzed separately by micro-CT and histomorphometry (supplemental online Fig. 2C).

### Histology and Histomorphometric Analysis

After micro-CT scanning and dehydration in descending alcohol series, we embedded the bone specimens without prior decalcification in low-temperature polymerizing methyl methacrylate (Merck Schuchardt OHG, Hohenbrunn, Germany; <http://www.merckmillipore.com/>), or we decalcified and embedded them in paraffin (see below). Longitudinal sections of 5  $\mu$ m thickness were prepared with a Jung K microtome (Reichert-Jung/Leica Microsystems, Wetzlar, Germany, <http://www.leica-microsystems.com>). Midsagittal histological sections of each biopsy were stained with Goldner's Trichrome to distinguish mineralized bone tissue (green) and unmineralized osteoid (red) [33]. The histological sections were divided in ROIs of 1 mm<sup>2</sup> for blinded histomorphometric analysis. Depending on the length of the biopsy, the number of ROIs ranged from 9 to 15. For each separate area of interest, we performed the histomorphometric measurements with a computer using an electronic stage table and a Leica DC 200 digital camera. The computer software used was Leica QWin (Leica Microsystems Image Solutions, Rijswijk, The Netherlands; <http://www.leica-microsystems.com/>). Digital images of the sections were acquired at 100 $\times$  magnification. A demarcation line was indicated between the “residual native bone” floor and the regenerated “graft-filled sinus” bone. Consecutive ROIs of 1 mm<sup>2</sup> each were defined and numbered throughout the whole biopsy. Data from the residual native bone part of the biopsy were pooled. Each ROI from the sinus floor toward the cranial side of the biopsy was analyzed separately. This method allowed us to compare similar ROIs for all biopsies (with and without stem cells) with respect to the bone regeneration in the augmented maxillary sinus, as indicated by the amount of osteoid and bone formed and the volume of remaining graft material. For each ROI, the bone volume (BV), graft volume (GV), and osteoid volume (OV) were calculated as a percentage of the total tissue volume (TV), as previously described [34].

### Statistical Analysis

Data are presented as mean  $\pm$  SD. Statistical analysis was performed with GraphPad Prism 4 software (GraphPad, La Jolla, CA, USA; <http://www.graphpad.com/>). Selected biopsies from bilaterally treated patients (with versus without SVF) were compared. It has been assumed that study and control sides were independent variables in bilaterally treated patients. An unpaired two-tailed Student's *t* test was performed to test differences between  $\beta$ -TCP and BCP in control samples. No

**Table 2.** Cell isolation data

Patient number	Adipose tissue volume (ml)	Total viable cell yield ( $\times 10^6$ )	Cells ( $\times 10^4$ ) per milliliter of adipose tissue	Viability (%)
1	150	30.5	20.3	94.1
2	240	33.8	14.1	88.0
3	305	41.5	13.6	86.4
4	320	85.1	26.6	80.1
5	240	41.3	17.2	88.4
6	220	28.0	12.7	81.4
7	220	42.3	19.2	81.3
8	320	79.9	25.0	77.6
9	220	35.9	16.3	76.8
10	290	55.7	19.2	74.8
Mean $\pm$ SD	253 $\pm$ 55	47.4 $\pm$ 20.1	18.4 $\pm$ 4.7	82.9 $\pm$ 6.1

Data on adipose tissue volume (in milliliters) was harvested and processed with a Celution 800/CRS device: the total viable cell yield ( $\times 10^6$ ), number of viable cells ( $\times 10^4$ ) per milliliter of adipose tissue, and the percentage of viable cells.

differences (clinically or statistically) were observed between control samples from both groups. Therefore, data of both groups were pooled, and a paired one-tailed Student's *t* test was performed to assess whether bone and osteoid volumes were higher and graft volumes lower at the study sides than at the control sides. Statistical significance was considered if *p* values were smaller than 0.05.

## RESULTS

### Clinical Evaluation and Implant Survival

The MSFE procedures with the use of calcium phosphates, seeded with the patient's own SVF in a one-step surgical procedure, were uneventfully performed, and all patients completed the study (supplemental online Fig. 1). During follow-up (>2.5 years), no clinically relevant changes were observed in general physical health of the patients and in blood laboratory measurements, nor were other adverse events related to the product or procedure. No dehiscence of the mucoperiosteal flaps nor any clinical signs of inflammation were observed postoperatively. All but one dental implant achieved good primary stability and appeared to be well osseointegrated after a healing period of 3 months. The one failing dental implant (patient 1, position 24) was painful, mobile, and disintegrated, and was therefore removed 1 month after dental implant insertion. However, this was unrelated to the stem cell product or the procedure; it was deduced that loss of the implant at position 24 was caused by premature loading of the implant by the temporary prosthesis. The patient underwent an autologous bone transplantation to restore bone to the indicated position of the lost dental implant.

### Radiological Evaluation

Panoramic radiographs were made prior to the MSFE procedure (supplemental online Fig. 3A) and after dental implant placement (*id est* 6 months post-MSFE) (supplemental online Fig. 3B). The gain in vertical bone height in the posterior maxilla on a panoramic radiograph at the planned dental implant positions requiring MSFE at the sides augmented with  $\beta$ -TCP was  $10.2 \pm 1.5$  mm (control sides), at the sides augmented with  $\beta$ -TCP and SVF was  $9.9 \pm 1.3$  mm (study sides) (supplemental online Fig. 3C, 3D),

at the sides augmented with BCP was  $12.4 \pm 1.6$  mm (control sides; *n* = 3 patients; six implant positions), and at the sides augmented with BCP and SVF was  $12.1 \pm 1.6$  mm (study sides; *n* = 5 patients; 10 implant positions) (supplemental online Fig. 3E, 3F). No significant differences were observed between study or control sides, nor within patients who were bilaterally treated using a so-called "split-mouth" design (patients 1–3, 6, 7, and 10) (Table 1). No clinical deviations were found on the panoramic radiographs nor on the cone beam CT scans (supplemental online Fig. 4).

### Cell Yield and Viability

Adipose tissue harvesting from the abdomen by liposuction resulted in  $253 \pm 55$  ml volume of adipose tissue as measured by the Celution/CRS800 device. Viability of the cells after isolation was  $82.9\% \pm 6.1\%$ , resulting in a total viable cell number of  $47.4 \pm 20.1 \times 10^6$  cells. The number of viable cells isolated per milliliter of adipose tissue was  $1.84 \pm 0.47 \times 10^5$  cells (Table 2). In all patients the cell product release criterion (>70% viability) was reached. Furthermore, in all 10 patients the total cell number was sufficient to allow seeding of a total of  $20 \times 10^6$  cells on 2 g of calcium phosphate carrier. Scanning electron microscopy and fluorescent nuclear staining on fixed surplus material confirmed the presence of cells attached to the calcium phosphate carrier (Fig. 2A, 2B).

### CFU-F Frequency and Cell Expansion

CFU-F assays were used to determine the frequency of cells with colony-forming capacity within the stromal vascular fraction. The mean frequency of cells with colony-forming capacity was  $1.4\% \pm 0.8\%$  (range, 0.1%–2.6%). After seeding of the cells for expansion at  $1 \times 10^5$  cells/cm<sup>2</sup>, 100% confluence was reached after  $5 \pm 1$  days. The mean cell yield was  $5.2 \pm 1.9 \times 10^5$  cells per  $1 \times 10^6$  SVF cells seeded. Using the cell yield and the percentage of initial cells with colony-forming potential, the population doubling time (PDT) was calculated (<http://www.doubling-time.nl>). The mean PDT was  $1 \pm 0.2$  days (range, 0.5–1.2 days), indicating that the initially seeded cells with colony-forming capacity underwent approximately five population doublings in 5 days.

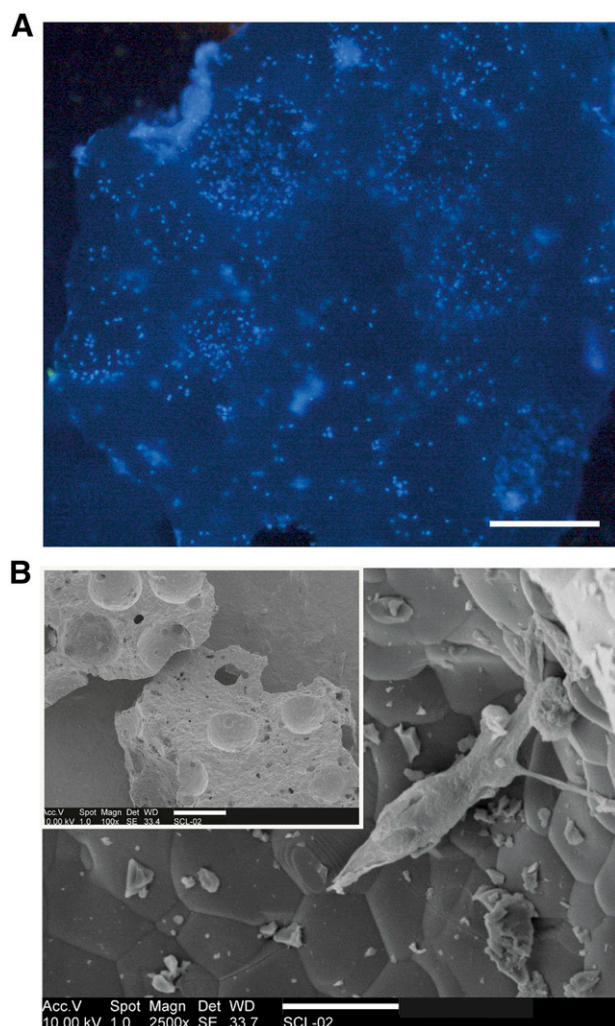


**Figure 2.** Cell seeding and attachment. **(A):** A representative image of calcium phosphate material seeded with stromal vascular fraction cells and fluorescently stained with 4',6-diamidino-2-phenylindole to visualize attached cells (blue) by fluorescence microscopy. Scale bar represents 200  $\mu\text{m}$ . **(B):** Scanning electron microscope image demonstrating attached cells on the calcium phosphate material (2500 $\times$  magnification). Scale bar represents 10  $\mu\text{m}$ . The inset is a representative scanning electron microscope image of the calcium phosphate granules at a lower magnification ( $\times 100$  magnification). Scale bar represents 200  $\mu\text{m}$ .

### Cell Surface Marker Profiling

To determine the phenotype of the SVF and cultured ASCs, we analyzed the cell surface marker profile. Expression of the markers was shown per donor, and the mean percentages of positive cells are shown for SVF cells (supplemental online Table 2) and ASCs (supplemental online Table 3). The surface marker expression on the SVF demonstrated a large subset of cells positive for CD29 (78%  $\pm$  11%), a cell adhesion marker, and the mesenchymal stem cell (MSC)-associated marker CD90 (83%  $\pm$  6%). A somewhat smaller population was positive for other MSC-associated markers, such as CD105 (21%  $\pm$  14%) and CD73 (37%  $\pm$  8%). A high percentage (67%  $\pm$  6%) of SVF cells was positive for hematopoietic stem cell and SVF-associated marker CD34, endothelial cell-associated marker

CD31 (47%  $\pm$  10%), and MHC molecules HLA-ABC (67%  $\pm$  6%) and HLA-DR (42%  $\pm$  80%). SVF cells were negative for CD117 and CD106. Furthermore, they were slightly positive for leukocyte marker CD45 (18%  $\pm$  5%), lineage cocktail 1 (Lin-1) staining lymphocytes, monocytes, eosinophils, and neutrophils (7%  $\pm$  2%), CD54 (36%  $\pm$  10%), and CD166 (16%  $\pm$  10%).

After 10–14 days of culturing the SVF cells, the attached ASCs were virtually all positive (97%–100%) for markers CD29, CD73, CD90, CD105, CD166, and HLA-ABC. No expression of CD45 or HLA-DR was found, and only in some of the ASC cultures did a minor population show expression of Lin-1 (6%  $\pm$  3%), CD117 (4%  $\pm$  5%), CD34 (4%  $\pm$  7%), CD31 (5%  $\pm$  3%), CD54 (51%  $\pm$  31%), and CD106 (6%  $\pm$  7%).

### Micro-CT Evaluation

The percentages BV/TV were higher in the selected biopsies from study sides than in those from control sides ( $\beta$ -TCP: 18.4%  $\pm$  6.8% vs. 11.2%  $\pm$  0.9%; BCP: 18.0%  $\pm$  2.4% vs. 16.2%  $\pm$  5.4%) (Fig. 3A, 3C). To gain more insight into where the bone was formed in the grafted area, ROIs from the residual native bone part of the biopsy were pooled, and ROIs from the maxillary sinus floor toward the cranial side of the biopsy were displayed separately (Fig. 3B, 3D). Bone in-growth was observed from the native residual alveolar bone of the maxillary sinus floor into the calcium phosphate-grafted area of the maxillary sinus. This de novo bone formation adjacent to calcium phosphate particles decreased from the pre-existing maxillary sinus floor toward the cranial side of the biopsies (Fig. 3B, 3D). Bone was found throughout the whole biopsies. In 8 out of 10 patients, bone was also present at the cranial side of the biopsies. Percentages GV/TV were comparable in study sides in comparison with the control sides ( $\beta$ -TCP: 9.7%  $\pm$  3.4% vs. 10.6%  $\pm$  3.4%; BCP: 12.1%  $\pm$  0.5% vs. 11.7%  $\pm$  2.3%) (Fig. 3E–3H). Pooled data for all biopsies, except those excluded as specified in the Materials and Methods section, are shown in supplemental online Figure 5.

### Quantitative Histomorphometric Evaluation

Higher BV/TV percentages were found for the selected biopsies from study sides compared with control sides ( $\beta$ -TCP: 16.4  $\pm$  5.2% vs 12.0  $\pm$  2.6%; BCP: 15.1  $\pm$  2.3% vs 14.7  $\pm$  3.2) (Fig. 4A, 4C). Similar to results from micro-CT analysis, the mineralized bone volume decreased from the residual native bone toward the cranial side of the biopsies, and was higher in the ROIs at the cranial side of the biopsies (Fig. 4B, 4D). More bone was found at the apical side (ROI 5-8) of the biopsies from the study sides ( $n = 7$ ) compared with control sides ( $n = 1$ ) (Fig. 4B, 4D). GV/TV was lower at the study sides compared with control sides ( $\beta$ -TCP: 17.4  $\pm$  9.4% vs 29.6  $\pm$  8.2%; BCP: 18.5  $\pm$  3.7% vs 19.1  $\pm$  5.9) (Fig. 4E, 4G), and this observation was seen in virtually all ROIs in the grafted area (Fig. 4F, 4H). OV/TV was significantly higher in the bone biopsies from study sides compared with control sides ( $\beta$ -TCP: 0.8  $\pm$  0.3% vs 0.2  $\pm$  0.1%; BCP: 0.9  $\pm$  0.8% vs 0.5  $\pm$  0.2) (Fig. 4I, 4K). The unmineralized osteoid volume was clearly more prominent in the newly formed bone area than in the residual native bone and higher in all ROIs throughout the grafted area (Fig. 4J, 4L). Pooled data for all biopsies, except those excluded as specified in materials and methods section, are shown in supplemental online Figure 6.

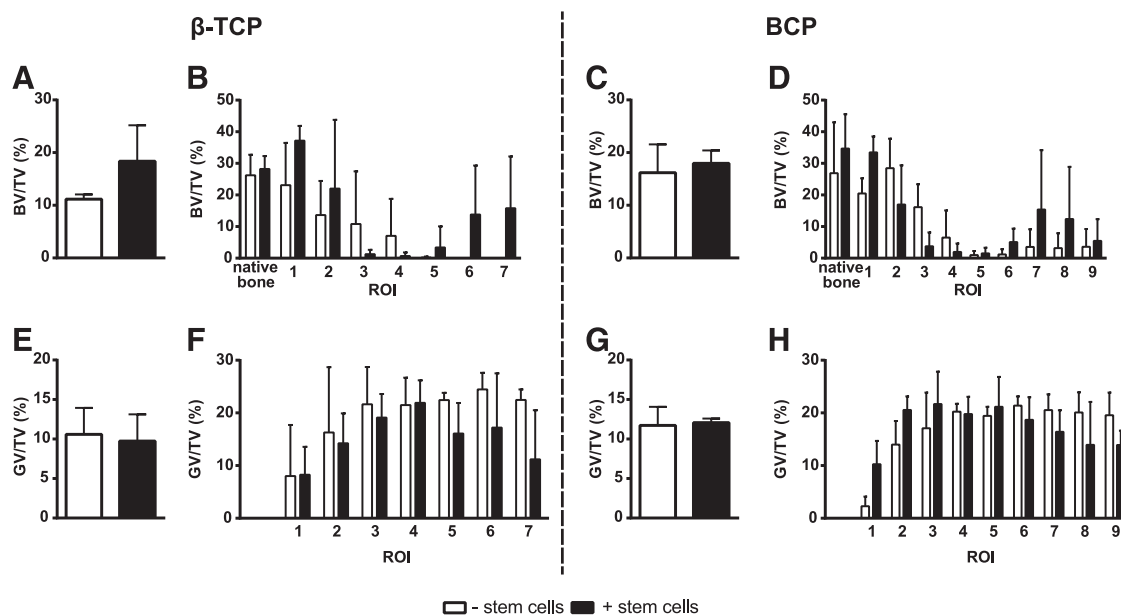


**Figure 3.** Micro-computed tomography analysis of selected bone biopsies taken from control sides without stem cells (white bars;  $n = 3$ ) and study sides with stem cells (black bars;  $n = 5$ ) from patients treated with  $\beta$ -tricalcium phosphate (A, B, E, F) or biphasic calcium phosphates (C, D, G, H). (A, C): Percentage mineralized BV/TV. (B, D): Percentage BV/TV in pooled native bone as well as per ROI. (E, G): Percentage GV/TV. (F, H): Percentage GV/TV in pooled native bone as well as per ROI. Data were shown only for ROIs  $n \geq 3$ . Abbreviations:  $\beta$ -TCP,  $\beta$ -tricalcium phosphate; BCP, biphasic calcium phosphates; BV, bone volume; GV, graft volume; ROI, region of interest; TV, total volume.

### Paired Analysis in Bilaterally Treated Patients

First, control samples from patients treated with  $\beta$ -TCP without SVF were compared with control samples from patients treated with BCP. No differences (clinically or statistically) were observed between control samples from patients treated with either  $\beta$ -TCP or BCP. Therefore, data of both calcium phosphates were pooled to enable paired analysis of study and control sides within bilaterally treated patients following a “split-mouth” design. Micro-CT analysis showed statistically significant higher BV/TV percentages at study sides than at control sides ( $19.5\% \pm 3.8\%$  vs.  $13.7\% \pm 4.4\%$ ;  $p = .03$ ) (Fig. 5A) and lower GV/TV percentages ( $10.5\% \pm 3.6\%$  vs.  $14.0\% \pm 3.6\%$ ;  $p = .07$ ) (Fig. 5B). Histomorphometric analysis showed higher BV/TV percentages in study sides in comparison with control sides ( $15.2\% \pm 4.7\%$  vs.  $13.3\% \pm 3.0\%$ ;  $p = .1$ ) (Fig. 5C); GV/TV percentages were lower in study sides than in control sides ( $17.7\% \pm 8.3\%$  vs.  $24.4\% \pm 8.6\%$ ;  $p = .1$ ) (Fig. 5D); and OV/TV percentages were higher in study sides than in control sides ( $0.6\% \pm 0.4\%$  vs.  $0.4\% \pm 0.2\%$ ;  $p = .06$ ) (Fig. 5E).

### DISCUSSION

The aim of this phase I clinical study was to assess the feasibility and safety of a one-step surgical procedure in the MSFE model using calcium phosphate (CaP) ceramics and freshly isolated SVF cells. Moreover, by performing inpatient comparisons of control and SVF-seeded augmentations in bilaterally treated patients (6 out of 10), we could assess the added value of SVF supplementation. In a previous study, it has been demonstrated that MSFE using  $\beta$ -TCP as a graft material is an effective treatment option, with high dental implant survival, regardless of the use of a resorbable collagenous barrier membrane to cover the lateral window [5]. On the basis of the latter study's results, the current study refrained from applying the membrane.

The one-step surgical procedure was shown to be feasible for MSFE. On average,  $2.5 \times 10^5$  nucleated cells per gram of tissue with a viability of 83% were obtained, well within the specifications of the Celution device. Because the mean colony-forming unit (CFU-F) frequency of the SVF isolates was 1.4%, and  $10 \times 10^5$  cells were seeded per gram of CaP,  $1.4 \times 10^5$  cells with CFU-F capacity were seeded per gram CaP. Cell attachment to CaP granules was confirmed by fluorescence staining and scanning electron microscopy.

The SVF surface marker expression profiles as determined with fluorescence-activated cell sorting were consistent with previous reports, including the CD34 positivity reported for ASCs, which is in contrast to the BMSC counterparts [22, 31, 32, 35]. Moreover, cultured ASCs showed a more homogeneous expression profile, *id est* they were positive for CD29, CD73, CD90, CD105, and HLA-ABC and lacked expression (or showed substantially declined levels) of CD31, CD45, CD34, and HLA-DR. The fact that expression of, for example, the hematopoietic markers such as Lin-1 can still be observed, although at a low level, can be explained by the early passage used to determine the cell surface marker expression.

The procedure was demonstrated to be safe for patients. All 10 patients were treated uneventfully, and no adverse effects were reported or detected in our large set of safety parameters (general health changes, physical examinations, radiological assessments, hematological parameters, and serum chemistry measurements (see the Materials and Methods section and supplemental Table 1 for a full description) until now, that is,  $\geq 3$ -year follow-up. The vertical bone/bone substitute height measured at the control sides and the study sides was sufficient to place the dental implants 6 months post-MSFE.

A striking observation from the histomorphometric and micro-CT analyses was the active bone formation observed at

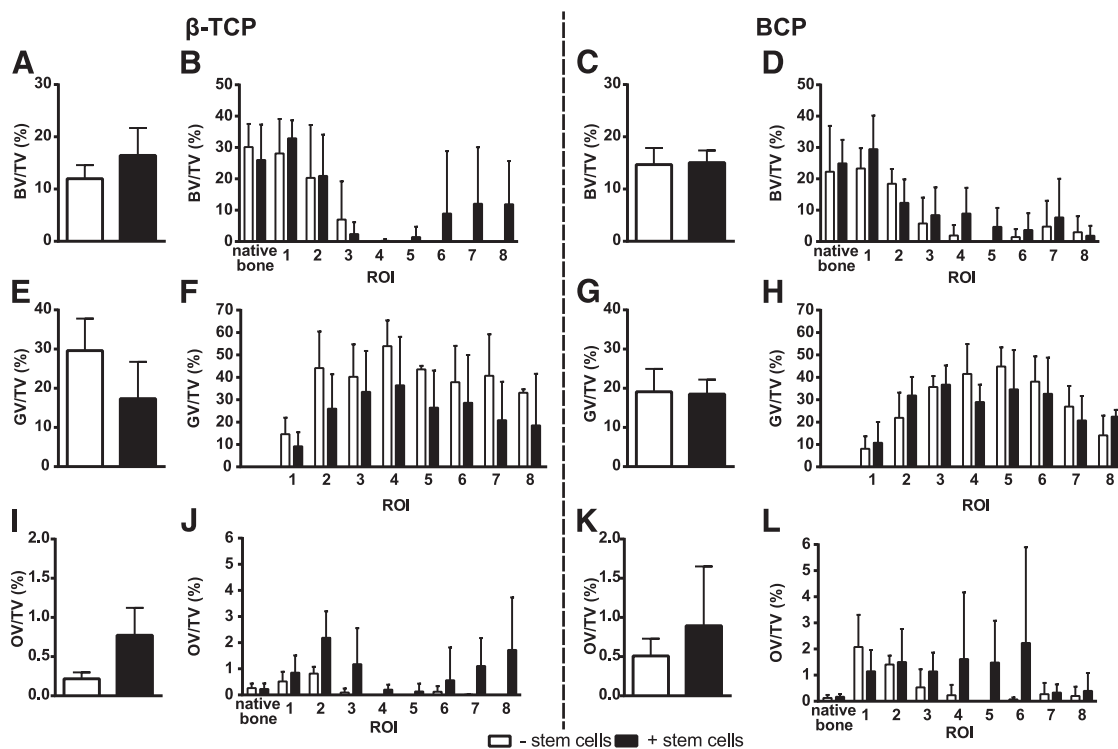


**Figure 4.** Histomorphometric analysis of selected bone biopsies taken from control sides without stem cells (white bars;  $n = 3$ ), and study sides with stem cells (black bars;  $n = 5$ ) from patients treated with  $\beta$ -TCP (A, B, E, F, I, J) or BCP (C, D, G, H, K, L). (A, C): Percentage mineralized BV/TV. (B, D): Percentage BV/TV in pooled native bone as well as per ROI. (E, G): Percentage GV/TV. (F, H): Percentage GV/TV in pooled native bone as well as per ROI. (I, K): Percentage unmineralized OV/TV. (J, L): Percentage OV/TV in pooled native bone as well as per ROI. Data were shown only for ROIs  $n \geq 3$ . Abbreviations: BCP, biphasic calcium phosphates; BV, bone volume; GV, graft volume; OV, osteoid volume; ROI, region of interest;  $\beta$ -TCP,  $\beta$ -tricalcium phosphate; TV, total volume.

the cranial side of the biopsies in 7 out of 10 of the selected bone biopsies taken from the study side, but only in 1 case from the control side. To our knowledge, this phenomenon has never been described before and may be unique to the current set-up. It may be due either to transdifferentiation of the ASCs within SVF toward bone-forming cells or to increased ASC paracrine recruitment of progenitor cells from the lateral bony window capping the bone reconstruction compartment. If the latter is true, this implies that it may be highly favorable to leave the lateral bony window of the maxillary sinus in situ. Currently, the extent of lateral bony window coverage of the bone substitute cranial surface is being tested in other clinical studies.

Surprisingly, a marked difference in bone formation in the grafted area was observed when comparing the BCP 60/40 and the  $\beta$ -TCP CaP scaffolds seeded with SVF, with the latter showing the highest bone volume content increase in comparison with their nonseeded (control) counterparts. Apparently, in line with numerous reports describing that numerous properties of CaP scaffolds—such as surface topography, crystallinity, grain and particle size, porosity, and chemical composition—may influence cell behavior [36], the choice of CaP type or producing company may markedly influence clinical outcome. Although the current study does not allow pinpointing which is the determining factor, this shows that any scaffold/SVF combination should be tested individually and that generalization is not allowed.

To gain more direct insight into the potential added value of SVF and to reduce biological heterogeneity effects, we conducted

paired analyses of control and SVF-seeded augmentations in bilaterally treated patients (6 out of 10). Even with this low number of patients, it could already be concluded that markedly higher bone contents ( $\mu$ CT:  $p = .03$ ; histomorphometry:  $p = .1$ ) were found in the grafted areas, which were supplemented with the freshly isolated SVF preparations. The same trend was observed for the percentage of osteoid volume within the grafted areas ( $p = .06$ ).

Interestingly, in each of the ROIs in the grafted area, the unmineralized osteoid percentages were higher at the study side than at the control sides, independent of the type of CaP used. This high content of osteoid, the prestage of mineralized bone formation, suggests that the SVF supplementation has markedly potentiated the bone-forming capacity in the augmented area and may result in higher bone volume following dental implant placement. Retrospectively, we might have opted for dental implant placement at an earlier time point—for example, after 4 months, as is routinely done for autologous bone [37]—to make optimal use of this potentiating effect of the SVF.

The use of a one-step surgical procedure using freshly isolated, autologous SVF (containing the stem/stromal cells, or ASCs) overcomes current limitations in other clinical studies using cultured mesenchymal stem cells for craniofacial bone reconstruction, such as the need for cell expansion in a costly GMP facility [38–43], the lack of inpatient controls [38–43], the need for ectopic bone formation [38, 42], a low number of patients treated for various craniofacial defects [41, 42], and multiple scaffold types either with or without growth factors

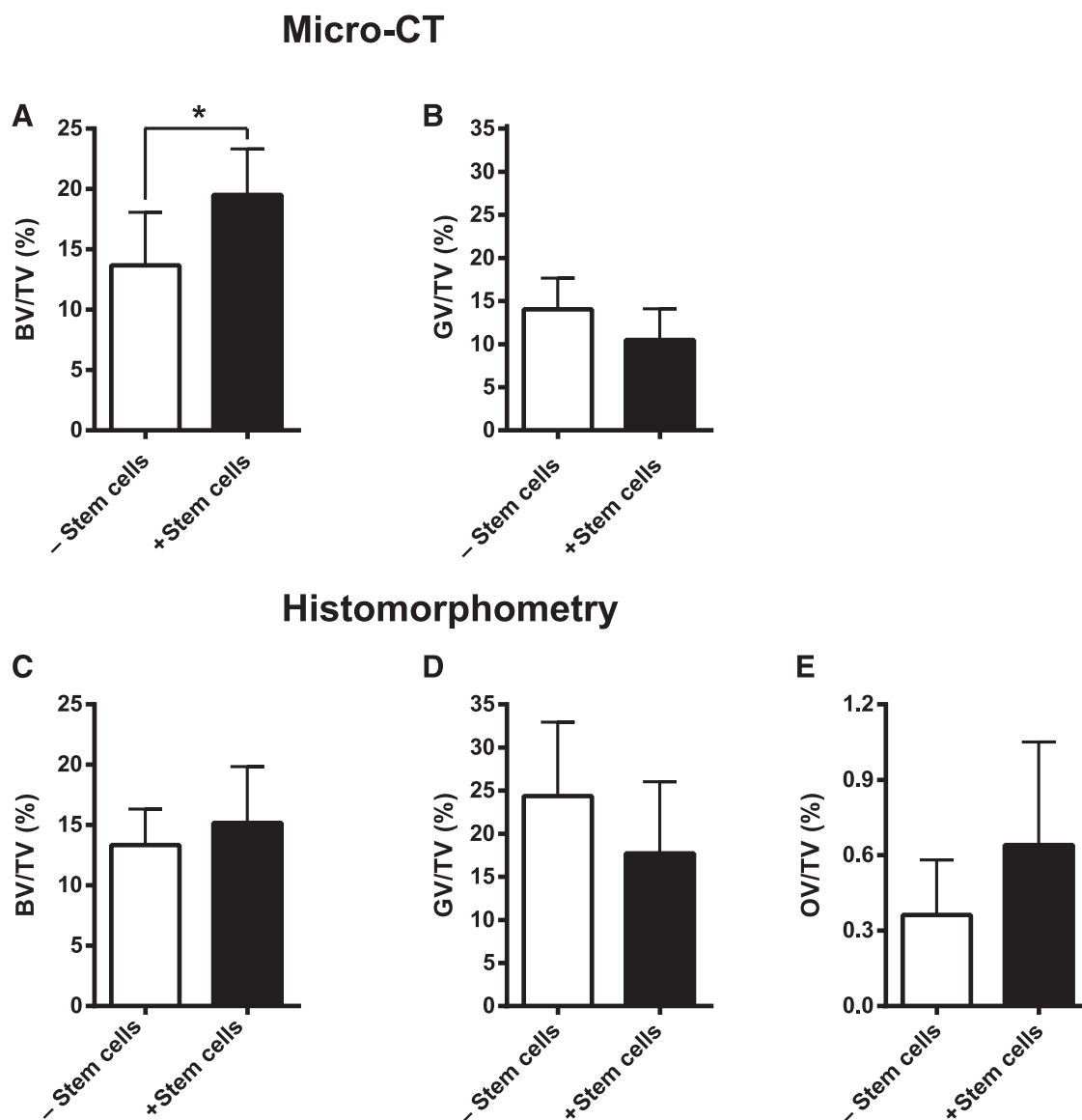


**Figure 5.** Paired micro-computed tomography (A, B) and histomorphometric analysis (C–E) of selected paired bone biopsies taken from control sides without stem cells and study sides with stem cells within the same patient following a “split-mouth design” ( $n = 6$ ). A paired one-tailed Student’s  $t$  test was performed to assess whether bone and osteoid volumes were higher and graft volumes lower at the study sides than at the control sides. \*Significantly different from control,  $p < .05$ . Abbreviations: BV, bone volume; CT, computerized tomography; GV, graft volume; OV, osteoid volume; TV, total volume.

[41]. The only clinical study applying freshly isolated SVF is a case report of a child suffering from widespread calvarial defects [44]. Although near complete calvarial continuity was achieved three months after the reconstruction, one has to keep in mind that a child has a very high regenerative capacity compared with the patients in our study. Moreover, the case report does not allow statements of the additive effect of SVF supplementation.

An experimental limitation of this study is the minor discrepancies in bone and graft volumes between histomorphometric results and micro-CT results, which could be attributed to experimental differences in two-dimensional and 3D measurements. Lower percentages of graft volume were observed by micro-CT analysis in comparison with histomorphometry throughout all grafted ROIs in biopsies with or without stem cells. This can be

explained by the fact that graft material was lost from the histomorphometrically examined sections, thus appearing as “massive” volumes, whereas the micro-CT measurements do take the pores within the scaffolds into account.

Another limitation of this study is that only one dosage of SVF (ASCs) was used. This dosage was chosen on the basis of feasibility, safety, and efficacy studies of the one-step surgical procedure using SVF in a goat spinal fusion model [45]. However, the encouraging initial efficacy data and complete absence of adverse effects of the current study certainly warrant further studies to evaluate whether higher dosages may show more effective bone formation without increasing side effects.

The maxillary sinus floor elevation (MSFE) model is unique because it allows biopsy collection without interfering with the clinical routine and inpatient treatment comparisons when using a

“split-mouth” design [29]. On the other hand, it is considered an area of relatively low biomechanical loading, which may dampen bone formation rate according to Wolff’s Law: “Use it or lose it” [46]. In preclinical studies, we have shown that the inclusion of a short (15 minutes) ex vivo stimulation of SVF with a physiological dose of bone morphogenetic protein-2 [25, 47, 48] or polyamines [49] results in upregulation of mature bone markers. Thus, it may be hypothesized that osteogenic “priming” improves osteogenic differentiation by the ASCs within the SVF, which may be particularly relevant in loading-compromised areas. Further preclinical in vivo studies are needed before clinical implementation can be considered, but it may be an appealing addition to the current concept.

The current study used full anesthesia, to avoid any complications during the procurement of the adipose tissue and the MSFE procedure. Although acceptable in a clinical trial format, the concept should be adapted to an outpatient setting with local anesthesia to render this concept cost-effective in the long run. Nevertheless, this first study using SVF in a one-step surgical procedure for bone regeneration certainly has potential and provides important cues for further studies on this novel concept.

## CONCLUSION

The results of this first clinical phase I study on the generation of bioactive implants, consisting of calcium phosphate carriers seeded with freshly isolated SVF during a one-step surgical procedure, demonstrated that the procedure is feasible and can be safely used in an MSFE procedure. Although the number of patients is limited, the efficacy data are encouraging. Future studies with more patients and higher cell doses might further improve efficacy and open new possibilities for a variety of cell-based bone tissue engineering applications.

## REFERENCES

- Rickert D, Slater JJ, Meijer HJ et al. Maxillary sinus lift with solely autogenous bone compared to a combination of autogenous bone and growth factors or (solely) bone substitutes. A systematic review. *Int J Oral Maxillofac Surg* 2012;41:160–167.
- Farré-Guasch E, Prins HJ, Overman JR et al. Human maxillary sinus floor elevation as a model for bone regeneration enabling the application of one-step surgical procedures. *Tissue Eng Part B Rev* 2013;19:69–82.
- Klijn RJ, Meijer GJ, Bronkhorst EM et al. A meta-analysis of histomorphometric results and graft healing time of various biomaterials compared to autologous bone used as sinus floor augmentation material in humans. *Tissue Eng Part B Rev* 2010;16:493–507.
- Zijderveld SA, Zerbo IR, van den Bergh JP et al. Maxillary sinus floor augmentation using a beta-tricalcium phosphate (Cerasorb) alone compared to autogenous bone grafts. *Int J Oral Maxillofac Implants* 2005;20:432–440.
- Schulten EA, Prins HJ, Overman JR et al. A novel approach revealing the effect of a collagenous membrane on osteoconduction in maxillary sinus floor elevation with  $\beta$ -tricalcium phosphate. *Eur Cell Mater* 2013; 25:215–228.
- Gimble JM, Bunnell BA, Guilak F. Human adipose-derived cells: an update on the transition to clinical translation. *Regen Med* 2012;7: 225–235.
- Grayson WL, Bunnell BA, Martin E et al. Stromal cells and stem cells in clinical bone regeneration. *Nat Rev Endocrinol* 2015;11: 140–150.
- Pittenger MF, Mackay AM, Beck SC et al. Multilineage potential of adult human mesenchymal stem cells. *Science* 1999;284: 143–147.
- Bernardo ME, Ball LM, Cometa AM et al. Co-infusion of ex vivo-expanded, parental MSCs prevents life-threatening acute GVHD, but does not reduce the risk of graft failure in pediatric patients undergoing allogeneic umbilical cord blood transplantation. *Bone Marrow Transplant* 2011;46:200–207.
- Duijvestein M, Vos AC, Roelofs H et al. Autologous bone marrow-derived mesenchymal stromal cell treatment for refractory luminal Crohn’s disease: Results of a phase I study. *Gut* 2010;59:1662–1669.
- Lucchini G, Introna M, Dander E et al. Platelet-lysate-expanded mesenchymal stromal cells as a salvage therapy for severe resistant graft-versus-host disease in a pediatric population. *Biol Blood Marrow Transplant* 2010;16:1293–1301.
- Bruder SP, Jaiswal N, Haynesworth SE. Growth kinetics, self-renewal, and the osteogenic potential of purified human mesenchymal stem cells during extensive subcultivation and following cryopreservation. *J Cell Biochem* 1997;64:278–294.
- Siddappa R, Licht R, van Blitterswijk C et al. Donor variation and loss of multipotency during in vitro expansion of human mesenchymal stem cells for bone tissue engineering. *J Orthop Res* 2007;25:1029–1041.
- Agata H, Asahina I, Watanabe N et al. Characteristic change and loss of in vivo osteogenic abilities of human bone marrow stromal cells during passage. *Tissue Eng Part A* 2010; 16:663–673.
- Rubio D, Garcia S, Paz MF et al. Molecular characterization of spontaneous mesenchymal stem cell transformation. *PLoS One* 2008;3: e1398.
- Izadpanah R, Kaushal D, Kriedt C et al. Long-term in vitro expansion alters the biology of adult mesenchymal stem cells. *Cancer Res* 2008;68:4229–4238.

## ACKNOWLEDGMENTS

This research was supported by ZonMW, the Netherlands organization for health research and development (project number 116001009). The authors thank Jolanda Hogervorst and Cor Semeins for technical assistance during stem cell preparations, Marion van Duin for excellent processing of the bone biopsies for histomorphometric analyses, Leo van Ruijven for help with the micro-computerized tomography analysis, Arie Werner for his technical assistance in scanning electron microscopy, Annelies Detmar and Arris Schuurkamp for help with all arrangements within the OR theater, and the plastic surgeons from the Department of Plastic Surgery of the Vrije Universiteit (VU) Amsterdam medical center for performing the liposuction procedures. H.-J.P. is currently affiliated with the Department of Hematology, VU University Medical Center, Amsterdam, The Netherlands.

## AUTHOR CONTRIBUTIONS

H.-J.P.: conception and design, collection and/or assembly of data, data analysis and interpretation, manuscript writing, final approval of manuscript; E.A.J.M.S.: conception and design, provision of study material or patients, collection and/or assembly of data, data analysis and interpretation, manuscript writing, final approval of manuscript; C.M.t.B.: conception and design, provision of study material or patients, collection and/or assembly of data, data analysis and interpretation, final approval of manuscript; J.K.-N.: conception and design, data analysis and interpretation, final approval of manuscript; M.N.H.: conception and design, collection and/or assembly of data, data analysis and interpretation, manuscript writing, final approval of manuscript.

## DISCLOSURE OF POTENTIAL CONFLICTS OF INTEREST

The authors indicated no potential conflicts of interest.

- 17** Zhu Y, Liu T, Song K et al. Adipose-derived stem cell: A better stem cell than BMSC. *Cell Biochem Funct* 2008;26:664–675.
- 18** Jurgens WJ, Oedayrasingh-Varma MJ, Helder MN et al. Effect of tissue-harvesting site on yield of stem cells derived from adipose tissue: implications for cell-based therapies. *Cell Tissue Res* 2008;332:415–426.
- 19** Katz AJ, Tholpady A, Tholpady SS et al. Cell surface and transcriptional characterization of human adipose-derived adherent stromal (hADAS) cells. *STEM CELLS* 2005;23:412–423.
- 20** Nakagami H, Morishita R, Maeda K et al. Adipose tissue-derived stromal cells as a novel option for regenerative cell therapy. *J Atheroscler Thromb* 2006;13:77–81.
- 21** Tholpady SS, Lull R, Ogle RC et al. Adipose tissue: Stem cells and beyond. *Clin Plast Surg* 2006;33:55–62, vi.
- 22** Varma MJ, Breuls RG, Schouten TE et al. Phenotypical and functional characterization of freshly isolated adipose tissue-derived stem cells. *Stem Cells Dev* 2007;16:91–104.
- 23** Faustini M, Bucco M, Chlapanidas T et al. Nonexpanded mesenchymal stem cells for regenerative medicine: Yield in stromal vascular fraction from adipose tissues. *Tissue Eng Part C Methods* 2010;16:1515–1521.
- 24** Jurgens WJ, Kroeze RJ, Bank RA et al. Rapid attachment of adipose stromal cells on resorbable polymeric scaffolds facilitates the one-step surgical procedure for cartilage and bone tissue engineering purposes. *J Orthop Res* 2011;29:853–860.
- 25** Overman JR, Farré-Guasch E, Helder MN et al. Short (15 minutes) bone morphogenetic protein-2 treatment stimulates osteogenic differentiation of human adipose stem cells seeded on calcium phosphate scaffolds in vitro. *Tissue Eng Part A* 2013;19:571–581.
- 26** Helder MN, Knippenberg M, Klein-Nulend J et al. Stem cells from adipose tissue allow challenging new concepts for regenerative medicine. *Tissue Eng* 2007;13:1799–1808.
- 27** Hoogendoorn RJ, Lu ZF, Kroeze RJ et al. Adipose stem cells for intervertebral disc regeneration: current status and concepts for the future. *J Cell Mol Med* 2008;12(6A):2205–2216.
- 28** Vergroesen PP, Kroeze RJ, Helder MN et al. The use of poly(L-lactide-co-caprolactone) as a scaffold for adipose stem cells in bone tissue engineering: Application in a spinal fusion model. *Macromol Biosci* 2011;11:722–730.
- 29** Pandis N, Walsh T, Polychronopoulou A et al. Split-mouth designs in orthodontics: An overview with applications to orthodontic clinical trials. *Eur J Orthod* 2013;35:783–789.
- 30** Tatum H Jr. Maxillary and sinus implant reconstructions. *Dent Clin North Am* 1986;30:207–229.
- 31** Naaijken BA, Niessen HW, Prins HJ et al. Human platelet lysate as a fetal bovine serum substitute improves human adipose-derived stromal cell culture for future cardiac repair applications. *Cell Tissue Res* 2012;348:119–130.
- 32** Prins HJ, Rozemuller H, Vonk-Griffioen S et al. Bone-forming capacity of mesenchymal stromal cells when cultured in the presence of human platelet lysate as substitute for fetal bovine serum. *Tissue Eng Part A* 2009;15:3741–3751.
- 33** Plenck H Jr. Bone tissue and teeth. In: Böck P, ed. *Romeis Microscopic Technique*. 17th ed. Munich, Germany: Urban & Schwarzenberg, 1989:527–566.
- 34** Parfitt AM, Drezner MK, Glorieux FH et al. Bone histomorphometry: Standardization of nomenclature, symbols, and units. Report of the ASBMR Histomorphometry Nomenclature Committee. *J Bone Miner Res* 1987;2:595–610.
- 35** Bourin P, Bunnell BA, Casteilla L et al. Stromal cells from the adipose tissue-derived stromal vascular fraction and culture expanded adipose tissue-derived stromal/stem cells: A joint statement of the International Federation for Adipose Therapeutics and Science (IFATS) and the International Society for Cellular Therapy (ISCT). *Cytotherapy* 2013;15:641–648.
- 36** Samavedi S, Whittington AR, Goldstein AS. Calcium phosphate ceramics in bone tissue engineering: a review of properties and their influence on cell behavior. *Acta Biomater* 2013;9:8037–8045.
- 37** van den Bergh JP, ten Bruggenkate CM, Tuinzing DB. Preimplant surgery of the bony tissues. *J Prosthet Dent* 1998;80:175–183.
- 38** Mesimäki K, Lindroos B, Törnwall J et al. Novel maxillary reconstruction with ectopic bone formation by GMP adipose stem cells. *Int J Oral Maxillofac Surg* 2009;38:201–209.
- 39** Thesleff T, Lehtimäki K, Niskakangas T et al. Cranioplasty with adipose-derived stem cells and biomaterial: a novel method for cranial reconstruction. *Neurosurgery* 2011;68:1535–1540.
- 40** Kaigler D, Avila-Ortiz G, Travan S et al. Engineering of maxillary sinus bone deficiencies using enriched CD90+ stem cell therapy: A randomized clinical trial. *J Bone Min Res* 2015;30:1206–1216.
- 41** Sándor GK, Numminen J, Wolff J et al. Adipose stem cells used to reconstruct 13 cases with cranio-maxillofacial hard-tissue defects. *STEM CELLS TRANSLATIONAL MEDICINE* 2014;3:530–540.
- 42** Sándor GK. Tissue engineering of bone: Clinical observations with adipose-derived stem cells, resorbable scaffolds, and growth factors. *Ann Maxillofac Surg* 2012;2:8–11.
- 43** Wolff J, Sándor GK, Miettinen A et al. GMP-level adipose stem cells combined with computer-aided manufacturing to reconstruct mandibular ameloblastoma resection defects: Experience with three cases. *Ann Maxillofac Surg* 2013;3:114–125.
- 44** Lendeckel S, Jödicke A, Christophis P et al. Autologous stem cells (adipose) and fibrin glue used to treat widespread traumatic calvarial defects: Case report. *J Craniomaxillofac Surg* 2004;32:370–373.
- 45** Kroeze RJ, Smit TH, Vergroesen PP et al. Spinal fusion using adipose stem cells seeded on a radiolucent cage filler: A feasibility study of a single surgical procedure in goats. *Eur Spine J* 2015;24:1031–1042.
- 46** Wolff J. *The Law of Bone Remodelling [Das Gesetz der Transformation der Knochen, 1892, P. Maquet & R. Furlong, trans.]*. Berlin, Germany: Springer Verlag, 1986.
- 47** Knippenberg M, Helder MN, Zandieh Doulabi B et al. Osteogenesis versus chondrogenesis by BMP-2 and BMP-7 in adipose stem cells. *Biochem Biophys Res Commun* 2006;342:902–908.
- 48** Overman JR, Helder MN, ten Bruggenkate CM et al. Growth factor gene expression profiles of bone morphogenetic protein-2-treated human adipose stem cells seeded on calcium phosphate scaffolds in vitro. *Biochimie* 2013;95:2304–2313.
- 49** Tjabringa GS, Vezeridis PS, Zandieh-Doulabi B et al. Polyamines modulate nitric oxide production and COX-2 gene expression in response to mechanical loading in human adipose tissue-derived mesenchymal stem cells. *STEM CELLS* 2006;24:2262–2269.



See [www.StemCellsTM.com](http://www.StemCellsTM.com) for supporting information available online.